

A 2D-PIV study and a numerical analysis of the natural convection in enclosures heated from below

FRANCESCO CORVARO, MASSIMO PARONCINI

Dipartimento di Energetica
 Università Politecnica delle Marche
 Via Brecce Bianche, 60100, Ancona
 ITALY

Abstract: - The aim of this paper is to determinate the influence of the position of a small heating source located in the bottom of a square cavity filled with air (Pr=0.71) on the natural convection flow structures and quantities (i.e. the distribution of the velocity vectors, the streamfunctions and the velocity fields). The experimental analysis was conducted through a 2D-PIV system. Two different positions are analyzed: one for a dimensionless distance from the left side of the enclosure of $\delta=0,4$ and another for $\delta=0,5$. The effects of the position of the hot strip are analyzed at different Rayleigh numbers: from $5 \cdot 10^4$ to $6 \cdot 10^5$. Then the results of the experimental PIV analysis were compared with the numerical results obtained with a finite volume code, Fluent 6.2.16, for both the geometrical positions of the heated strip.

Key-Words: - Natural convection; PIV technique; Numerical analysis.

Nomenclature

d position of the heat source (m)
 g modulus of the gravity vector ($g=9.81 \text{ m s}^{-2}$)
 H square cavity side (m)
 k thermal conductivity ($\text{W m}^{-1} \text{ K}^{-1}$)
 l heat source length (m)
 L cavity depth in the experimental tests (m)

Pr $\frac{\nu}{\alpha}$ Prandtl number
 Ra $\frac{g\beta H^3(T_h - T_c)}{\nu\alpha}$ Rayleigh number

T temperature (K)
 T $\frac{(T_h + T_c)}{2}$ average temperature (K)
 ΔT $(T_h - T_c)$ temperature difference between heat source and cold plate (K)

x, y Cartesian coordinate
 X, Y $\frac{x}{H}, \frac{y}{H}$ dimensionless Cartesian coordinate

Greek Letters
 δ $(d + \frac{l}{2}) / H$ dimensionless position of the heat source

ε $\frac{l}{H}$ dimensionless length of the heat source

θ $\frac{(T - T_c)}{(T_h - T_c)}$ dimensionless temperature

ν kinematic viscosity ($\text{m}^2 \text{ s}^{-1}$)
 ρ density (kg m^{-3})

Subscripts

c cold wall
 h hot wall

1 Introduction

The natural convection in a square cavity has a very interesting role in a lot of engineering applications, such as solar energy system, cooling of the electronic circuits, conditioning of the air and many others, therefore it plays an important role in the applied research. Technical literature presents a lot of studies on natural convection in a square cavity and many of them analyze the convective phenomenon thanks to numerical simulation. Valencia and Frederick [1] elaborated a numerical investigation on the heat transfer of air in square cavities with partially active vertical walls. Aydin et al. [2] simulated numerically the natural convective heat transfer in air in a square cavity cooled from the side walls and heated by a strip placed at the center of the bottom wall. Nibarufata et al. [3] analyzed numerically the natural convection in partitioned enclosures with a localized heating from below. Ramos and Milanez's [4] paper treats the natural convection in cavities heated from below by a thermal source, which dissipated energy at a constant rate.

In this paper the cavity testing is a square enclosure and we analyzed the influence of the position of the heated strip on natural convection heat transfer; the heated strip was placed on the bottom of the cavity. Two different dimensionless positions of the hot strip are analyzed: $\delta=0,4$ and $\delta=0,5$. The dimension of the heat brass is $\varepsilon=0,2$ of the side of the cavity. The cavity is cooled from the side walls at the same time and it is filled with air. The dynamic convective structures are analyzed through a 2D Particle Image Velocimetry. With this experimental equipment we evaluated the distribution of the velocity vectors, the streamfunctions and the velocity fields. Moreover the PIV results were compared with the results of the numerical analysis obtained with a finite volume code: Fluent 6.2.16. The experimental research analyzed different Rayleigh numbers in particular from $5 \cdot 10^4$ to $6 \cdot 10^5$ while with the numerical study we expanded this range from $5 \cdot 10^4 < Ra < 6 \cdot 10^5$ to $3 \cdot 10^4 < Ra < 9 \cdot 10^5$ after a first comparison between the numerical and experimental results.

2 Experimental apparatus

The main components of the experimental apparatus, represented in Fig.1, include the test cell, filled with air at atmospheric pressure, the PIV system, two thermostatic baths with their hydraulic circuits and the data acquisition system.

The Particle Image Velocimetry (PIV) is finalized to make instantaneous velocity measurements in the cross-section of a flow. The PIV system provides the velocity fields by the distance made by the particles-seeded in the flow. The seeding particles nature must be chosen in order to provide a real description of the air flow. In this experiment the nebulized oil particles have a diameter of about 1 μm . The laser used is a double cavity Nd-Yag laser with a wavelength of 532 nm.

The data analysis was performed using the software package "Flow Manager", provided by Dantec Dynamics (2000).

The images of the area of the flow field, lighted by a light-sheet, are captured by a CCD camera (Hamamatsu camera C8484-05C with 1344×1024 number of pixels). The camera lens was covered by a filter with a wavelength $\lambda=532$ nm in order to record only the direct or scattered light from the laser source inside the PIV cavity.

The test-cell, shown in Fig.2, has a square transversal section of $H=0,05$ m. The brass heat source is positioned on the lower horizontal wall

and it has a temperature T_h , maintained constant through the continuous circulation of thermostatic fluid in the thermostatic bath.

The lateral vertical walls, that are made up of aluminum, are cooled by a fluid which is cooled by another thermostatic bath at a uniform temperature T_c .

The light-sheet gets in through the upper part of the enclosure made up of plexiglas and it lights up a cross section of the cavity in the middle of the cell. The camera, that is located perpendicularly to the light-sheet, captures the images, which are sent to a computer to be processed.

The front sidewall of the cavity is covered by a small pane of glass to permit an optical access to the camera; instead the rear side is rigged with a 0.05 m square piece of wood which has an opening in the centre. Through it we sprinkle the oil particles 20 s before the beginning of each test. The top and the bottom surfaces of the enclosure are made up of plexiglas with a thickness of 0,03 m to neglect the leaks of heat through these surfaces.



Fig.1 Experimental apparatus

The test-cell dimension along the longitudinal direction is 0,41 m. It is greater enough than H to neglect the air motion along the z axis so it is possible to ignore the end effect and to consider the problem as a two-dimensional one.

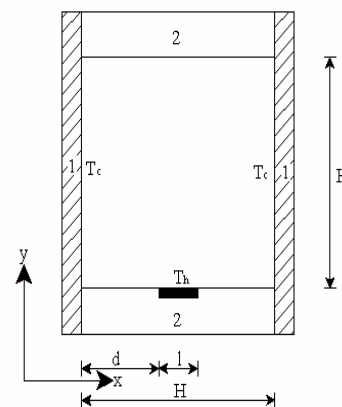


Fig.2 Test cell

The temperatures of the test-cell are measured through copper-constantan thermocouples.

Ten thermocouples are positioned on the surfaces of the cool lateral walls and three of them are located on the brass surface of the heat source.

The difference among the three values of the temperature on the brass plate is less than 0,1 K therefore the situation can be considered isotherm, the maximum difference among the five thermocouples of the lateral wall is 0,5 K.

The Rayleigh numbers analyzed change from $5 \cdot 10^4$ to $6 \cdot 10^5$.

In the tests performed with the PIV technique, the time between the two different laser pulses is set depending on the Ra number and on the position of the heating source as it is summed up in table 2 (as far as the symmetrical configuration) and in table 1 (as far as the asymmetrical configuration). This choice is made in order to have a better signal to noise ratio.

$\delta=0,4$	
Ra	Δt [μs]
1,3E+05	10500
1,6E+05	9000
2E+05	8100
2,3E+05	7400
2,5E+05	7000

Table 1. Times between two different laser pulses for the asymmetrical configuration

$\delta=0,5$	
Ra	Δt [μs]
1,3E+05	8500
1,6E+05	8000
2E+05	7000
2,3E+05	5000
2,5E+05	4000

Table 2. Times between two different laser pulses for the symmetrical configuration

The processing technique used in this study is Dantecs' cross-correlation, described by Dantec Dynamics (2000) [5], with an interrogation area of 32x32 pixels.

The overlap of the interrogation area in the horizontal and vertical direction is 50%. Furthermore a moving average validation is applied; this method validated vectors based on comparison

between neighboring vectors: an averaging area of 3x3 is used with an acceptance factor of 0.1 and there are 3 iterations. This method substituted outliers due to false correlations resulting from reflections at the cell walls and the other invalid vectors.

3 Numerical procedure and setting

The Fluent solution methods are known in the scientific background and a detailed description of the mathematical model can be found in the Fluent User's Guide [6].

The numerical simulation is developed with the finite volume code Fluent 6.2.16 using the Boussinesq approximation for air and a two-dimensional model.

The numerical results are carried out with the segregated solvers [6] for $3 \cdot 10^4 < Ra < 9 \cdot 10^5$.

In the analysis performed thanks to the software the cavity was reproduced with the real dimensions, and the temperature of the lateral walls and of the heated strip is assigned in order to obtain the analyzed Rayleigh number as in the experimental analysis.

A uniform mesh structure with a square cell is performed. A study of the mesh was carried out preliminarily to obtain the lowest number of cells necessary to perform an analysis with results which are independent from the choice of the cell number. Appreciable changes have not been observed in results with a mesh of over 22500 cells. For example, for a $Ra = 1 \cdot 10^5$ the increase of the mesh size from 150x150 to 200x200 produces a change in the average velocity inside the cavity of about 0.54%. We tried to use a mesh refinement near the walls but, also in this case, relevant improvements in the accuracy of the results were not observed. So we chose to work with a uniform mesh structure of 22500 cells.

Steady and unsteady solvers are both used in the analysis; in the steady procedure the admitted value for all residuals to obtain convergence is 10^{-5} , while in the unsteady technique the admitted value for the convergence is 10^{-11} .

The unsteady procedure allows the analysis of the possible periodicities or instabilities in the motion. The dimensionless time step used vary from 10^{-4} to 10^{-6} , and the number of time steps has been chosen sufficiently high to have an asymptotic steady-state solution. In the unsteady solvers the maximum number of iterations per time step is generally high enough to reach the grid limit of calculation with a constant value for all the residuals.

The velocity fields, the streamfunctions and the velocity vectors distribution inside the cavity obtained numerically were compared to the experimental results.

4 Results and discussion

During the experimental analysis we observed as the convective motion develops in the air inside the cavity as soon as the hot fluid begins to circulate through the strip.

When the strip begins to warm it is possible to observe as the displacement of the air creates two big vortexes as showed in Fig.5.

When the strip is located in a symmetrical position, $\delta=0.5$ (Fig.5), the convective cylinders are symmetrical.

Moreover if we observe Fig.5b the streamfunctions show that these two vortexes rotate in the opposite directions. This effect doesn't change even if we change the geometrical configuration as we can notice in Fig.5b.

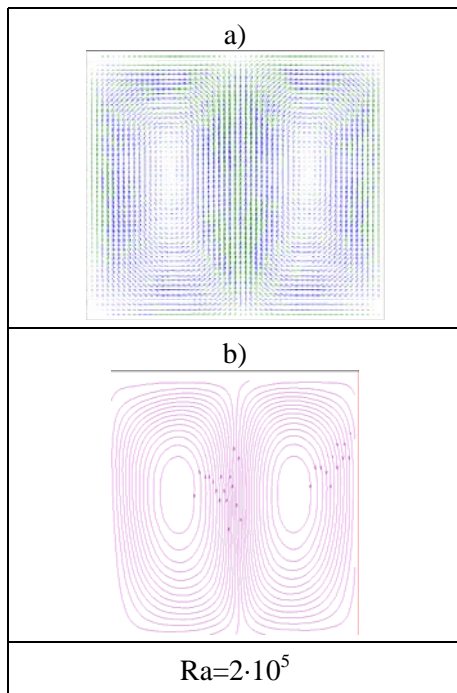


Fig.5 Experimental Data: Vector map and stream function for $\delta=0,5$

These behaviors are also confirmed in the numerical analysis as showed in Fig.6 where we can find again the same distribution of the streamfunctions.



Fig.6 Numerical streamlines for $\delta=0.5$ ($Ra=2 \cdot 10^5$)

In the second geometrical configuration, where the hot strip is not in the centered position but it is at $\delta=0.4$, the left convective cylinder begins to become smaller than the right one so the compression in the air flow development begins. It is not present a symmetrical configuration and the contact line of the two vortexes moves in the left part of the cavity as it is showed in Fig.7b.

This phenomenon is also confirmed in the numerical analysis as showed in Fig.8.

Fig.5a and Fig.7a represent the distribution of the velocity vectors inside the enclosure with different configurations.

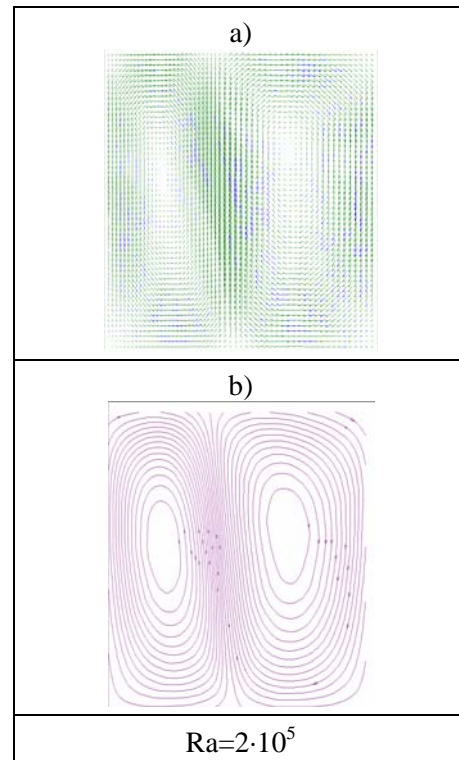


Fig.7 Experimental Data: Vector map and stream function for $\delta=0,4$



Fig.8 Numerical streamlines for $\delta=0.4$ ($Ra=2 \cdot 10^5$)

These aspects are not influenced by the Rayleigh number. In fact the variations of the Rayleigh number don't create changes in the streamfunctions or in the distribution of the velocity vectors. Instead strong relationship between the Rayleigh number and the modulus of the velocity vectors was found in the experimental analysis and it was confirmed by the numerical results. If we observe Fig.9 and 10 we can see as the velocity fields increase with the Rayleigh number.

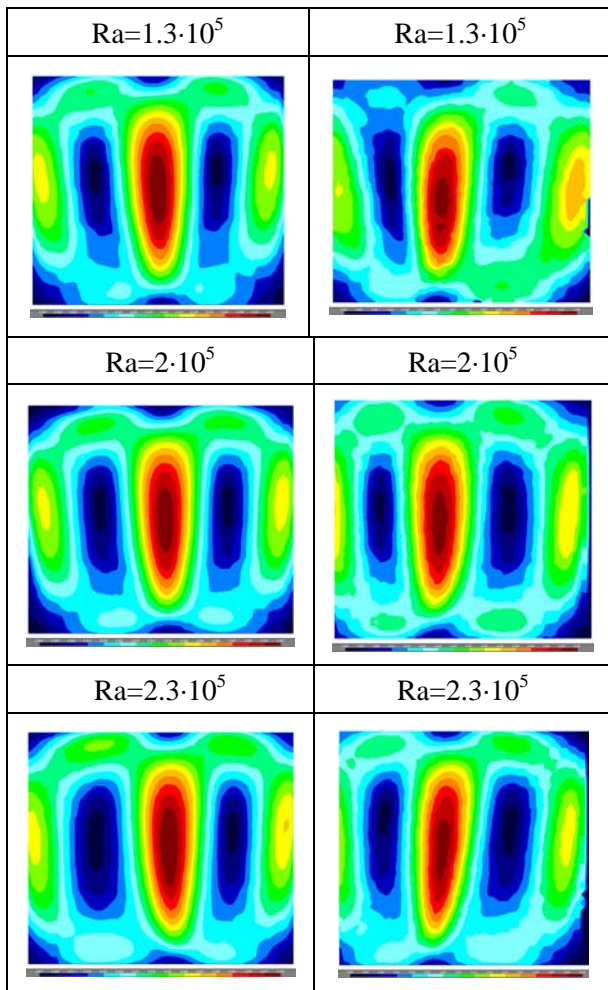
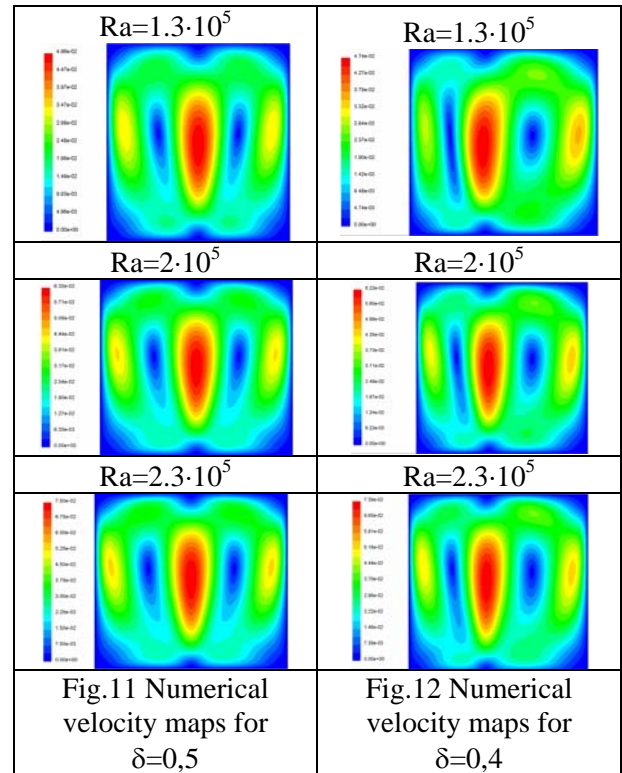


Fig.9 PIV velocity maps for $\delta=0,5$

Fig.10 PIV velocity maps for $\delta=0,4$

Moreover the non symmetrical configuration shows an average flow field slower than the symmetrical one. This effect is probably connected with a better natural convection generated in the symmetrical configuration. The increasing of the natural convection in symmetrical configurations creates a faster velocity field in the air inside the cavity.



Finally in Fig. 11 and 12 it is possible to observe the numerical results. They confirm the experimental analysis: the velocity field increases with the Rayleigh number and the symmetrical configuration has a quicker velocity field than the asymmetrical one.

Moreover we can also see a good agreement between the numerical values and the experimental ones even when we consider the quantitative aspect. In fact if we compare the maximum velocity values obtained in the numerical analysis – Fig.11 and Fig.12 – and in the experimental study - Fig.9 and Fig.10 – we find a maximum percent deviation of 6,8% for $Ra=2 \cdot 10^5$ in the symmetrical configuration while for the average velocity it is of 3,58%.

5 Conclusion

In the paper it was analyzed the influence of the heat source position on the natural convective heat transfer in a square cavity.

The analysis was conducted experimentally, with Particle Image Velocimetry (PIV), for a Rayleigh number with a variation range from $5 \cdot 10^4$ to $6 \cdot 10^5$. The PIV analysis gives us flow structures connected with the convective phenomenon like the velocity fields, the streamfunctions and the velocity vector distributions.

The experimental analysis is connected to the numerical analysis that was made through a simulation code with Ra number range of $3 \cdot 10^4 < Ra < 9 \cdot 10^5$.

The configuration with the heat source located centrally shows a symmetrical development of the phenomenon and therefore a symmetrical distribution of the velocity field that increases with the Rayleigh number.

With the PIV technique we can observe two recirculating zones: two convective cylinders that changes with the geometrical configuration. In fact one of these two vortexes, the left one is compressed on the lateral wall in the second configuration ($\delta=0,4$).

This relevant configuration also causes a decrease in the convective heat transfer and consequently in the velocity fields. In fact both the experimental data and the numerical one show as the velocity fields increase with the Rayleigh number.

Moreover in the symmetrical configuration, at the same Rayleigh number of the asymmetrical one, a faster velocity field can be observed.

References:

- [1] X1. A. Valencia and R. L. Frederick, Heat transfer in square cavities with partially active vertical walls, *Int. J. Heat Mass Trans.*, Vol.32, No.8, 1989, pp. 1567-1574.
- [2] X1. O. Aydin and W. J. Yang, Natural convection in enclosures with localized heating from below and symmetrical cooling from sides, *Int. J. Num .Methods Heat Fluid Flow*, Vol.10, No. 5, 2000, pp. 519-529.
- [3] X1. E. Ntubarufata, M. Hasnaoui, E. Bilgen and P. Vasseur, Natural convection in partitioned enclosures with localized heating, *Int. J. Num. Meth. Heat Fluid*, Vol.3, No.X, 1993, pp. 133-143.
- [4] X1. R. A. V. Ramos and L. F. Milanez, Numerical and experimental analysis of natural convection in cavity heated from below, Proc. 11th IHTC Kyongju, Korea, Vol.3, 1998.
- [5] X1. FlowManager software and Introduction to PIV Instrumentation, Dantec Dynamics GmbH, Publication number: 9040U3625 (2000).
- [6] X1. Fluent User's Guide, release 6.2.16, Fluent Incorporated (2005-01-06).
- [7] X1. M. Bourich, M. Hasnaoui, A. Amahmid, Double-diffusive natural convection in a porous enclosure partially heated from below and differentially salted, *International Journal of Heat and Fluid Flow* 25 (6) (2004), pp. 1034-1046.
- [8] X1. M.M. Ganzarolli, L.F. Milanez, Natural convection in rectangular enclosures heated from below and symmetrically cooled from the sides, *International Journal of Heat and Mass Transfer*, 38 (6) (1995), pp. 1063-1073.
- [9] X1. T.Y. Chu, C.E. Hichox, Heat convection with large viscosity variation in an enclosure with localized heating, *International Journal of Heat Transfer*, 112 (1990), pp. 388-395.
- [10] X1. G. Cesini , M. Paroncini, G. Cortella, M. Manzan , Natural convection from a horizontal cylinder in a rectangular cavity, *Int. J. Heat and Mass Transfer*, Vol.42,1999, pp.1801-1811.